COMPARISON OF THREE MAGNETIC RESONANCE IMAGING SEQUENCES FOR MEASURING CARTILAGE THICKNESS IN THE CANINE STIFLE

by

Lawrence Alexander Brown

A thesis submitted to the Graduate Faculty of
Auburn University
in partial fulfillment of the
requirements for the Degree of
Master of Science

Auburn, Alabama
August 4, 2012

Approved by

Merrilee Holland, Chair, Department of Clinical Sciences
Judith Hudson, Department of Clinical Sciences
John T Hathcock, Department of Clinical Sciences
Calvin Johnson, Department of Pathobiology

Abstract

Magnetic Resonance Imaging (MRI) using 3 sequences; Proton Density Spin Echo (PDSE), 3 Dimensional Spoiled Gradient with Fat Suppression (3D SPGR-FS) and Steady State Free Precision (SSFP) in the sagittal plane was carried out on 11 normal cadaver stifles. The stifles were imaged within 24hrs postmortem. Three readers obtained cartilage thickness measurements from the images of all sequences. These measurements were compared to those obtained from histological prepared specimens in the sagittal plane. Histology specimens were prepared from the location where MRI images had been obtained. The values for mean cartilage thickness from MRI and histology were compared using regression, correlation, and student's t test. Pearson's Correlation was used to assess correlation of cartilage thickness values obtained from magnetic resonance images and histology as well as to assess correlation among readers. There was no significant difference between MRI and histology measurements in 20.2% of the images combined for all sequences. Of these, the Balanced Steady State Free Precision (BSSFP) sequence had the highest number of images that were not significantly different from the histologic measurements (24%). MRI measurements generally overestimated cartilage thickness when compared to histology. There was moderate correlation between histology measurements and MRI images for all readers (R values: 0.25 to 0.77). Correlation between readers for all sequences varied from moderate to poor (R values: 0.25 to 0.77). There was poor coefficient of variations for all image types when compared to histology. All sequences had sufficient contrast resolution to identify the articular cartilage of the femoral condyles. Further investigation of

these sequences using a higher field strength magnet may allow more accurate evaluation of cartilage thickness by allowing further manipulation of the matrix size and field of view to more accurately represent cartilage thickness in the canine stifle.

Acknowledgments

The author would like to thank Dr. Merilee Holland and Dr. Judith Hudson for their patience in carrying out this project. He would also like to thank Dr. John T. Hathcock for his time spent contributing to the results. A special thanks go to Dr. Calvin Johnson for his time and help explaining the histology preparation techniques. Thanks also go to Dr. James Wright for his time performing the statistical analysis and explaining the results.

This project would not have been possible without the technical assistance of Kim Bryan and Terrell Lynch; thank you both.

The author also wished to acknowledge the support of his mother Sandra, brother Nicholas for their endless support and sacrifices. I would not be where I am if it were not for you both. The support of Dr. Lauren Reid over the last few years, in good times and bad, has been invaluable.

Table of Contents

List of Figures

I. INTRODUCTION

Osteoarthritis (OA) and other diseases affecting the cartilage in the stifle joint of small animals can dramatically affect their quality of life. It is the most common arthropathy in the dog.[10] Great emphasis has been placed on non-invasive evaluation of cartilage in human medicine, where the disease processes are similar to those in veterinary patients. Evaluation of cartilage thickness is an important indicator for staging arthritic disease. Studies have been conducted on horses to evaluate the accuracy of magnetic resonance imaging for estimating cartilage thickness;[1] however, little research has been published for small animals.

The project goal was to assess the diagnostic value of three magnetic resonance imaging sequences, currently used in human medicine, for imaging the canine stifle. The plan was to compare and contrast the ability of these sequences to allow accurate assessment of cartilage thickness in canine stifle cadaver specimens. Measurements of cartilage thickness from each image sequence were made at standardized locations on the femoral condyles. These values were compared to measurements of cartilage thickness obtained from gross dissection and histological analysis of the stifle joints. Statistical analysis using correlation and the student's t test were carried out to compare MRI measurements of cartilage thickness with those from histological sections.

From the results of this study, the goal was to find an MRI sequence which can be used to accurately assess cartilage thickness, and therefore recommend a magnetic resonance imaging sequence and technique that can be added to a standard stifle imaging protocol to best evaluate cartilage degeneration with canine stifle disease.

This study tested the following hypotheses:

1. Cartilage thickness in dogs measured using MRI is similar to that measured using histopathology.
2. There is no difference in measurements of cartilage thickness obtained using 3 techniques: Proton Density Spin Echo (PDSE), 3 Dimensional Spoiled Gradient with Fat Suppression (3D SPGR-FS) and Steady State Free Precision (SSFP).

Specifically, the study sought to assess the ability of three MRI sequences to accurately cartilage thickness in the canine stifle joint and to determine if there is any significant difference between the accuracy of the three sequences.

II. LITERATURE REVIEW

Lameness is a common clinical presentation in small animal medicine. A common cause of lameness is degenerative joint disease, which includes chronic changes to the cartilage, joint capsule and synovium.[2]

Typically, degenerative joint disease is diagnosed in small animal patients using the combination of a complete history, physical exam and radiographs of affected joints. Radiographs are excellent at evaluating bone; however, they are extremely poor at allowing cartilage assessment. Clinicians and students at veterinary schools are taught to evaluate radiographs for secondary changes associated with cartilage abnormalities, e.g. narrowing of joint spaces, osteophyte formation and subchondral bone changes. Contrast arthrography can be used to evaluate surface defects, but without invasive arthroscopic procedures or surgical techniques, joint cartilage cannot be directly evaluated.

Magnetic Resonance Imaging (MRI) is used in human orthopedic medicine to evaluate cartilage pathology in joint disease[3,5,7]. This modality - like radiography and computed tomography - is a non-invasive imaging technique; however, it differs by using the concepts of magnetic induction and magnetic resonance to form multiple 2D images with excellent soft tissue contrast. This allows evaluation of both bone and soft tissue structures and contributes to the understanding of the pathophysiology for joint diseases.

Degenerative joint disease leads to a decrease in the thickness of articular cartilage. Therapy for this disease process attempts to slow down the rate of degeneration by direct or indirect means. Therapies in small animal medicine include weight control, physical therapy and pharmaceutical / neutraceutical use. Owners and clinicians evaluate patient response through

activity levels, pain and body condition score improvement and radiographic assessment of affected joints. The response of cartilage to therapy is not evaluated directly.

If an MRI protocol that allows accurate and precise measurement of cartilage thickness can be defined, we would have a method to directly evaluate progression of degenerative joint disease and possibly to determine the efficacy of various treatment options over time. This point is echoed in current human literature where it has been stated that MRI imaging of cartilage may allow for large scale studies of OA progression to be conducted, as well as clinical trials for investigating the efficacy of structure modifying OA drugs.[3]

MRI research on cartilage evaluation in veterinary medicine is limited compared to human medicine. There has been recent interest in Large Animal (LA) medicine for investigating the ability of this modality to evaluate cartilage. A 2010 study[1] evaluated MRI in its ability to assess osteoarthritis in the metacarpophalangeal joint of standardbred and thoroughbred racehorses. Twenty cadaver legs were imaged at the level of the metacarpophalangeal joint using MRI with a single pulse sequence. Specific locations in the joint were selected to evaluate correlation between MRI images and gross measurements. This study reported good precision and moderate correlation ($r = 0.44$; $p < 0.0001$) between of the two methods of measuring cartilage thickness.

In a similar 2005 study,[4] 32 horse cadaver legs were imaged at the level of the carpal joint using two different pulse sequences. Cartilage thickness measurements of the radial, intermediate and ulnar carpal bones from these sequences were compared with gross measurements. Significant correlation ($r=0.96$; $P<0.001$) was reported between the images from different pulse sequences and gross measurements; however, variation between MRI and gross thickness depended on whether or not the histology measurement included the calcified cartilage

layer. When the calcified cartilage layer was not included, MRI measurements were significantly greater than gross measurements suggesting that MRI better estimates cartilage thickness when measurements include the calcified cartilage layer.

A number of studies have been carried out in human medicine comparing the ability of various pulse sequences to evaluate cartilage thickness in assorted joints. An extensive review of MRI cartilage imaging protocols was presented by the Osteoarthritis Research Society International in 2006[3]. This review concluded that high accuracy and adequate precision for quantitative assessment of cartilage morphology can be obtained using fat-suppressed gradient echo MRI sequences, and appropriate image analysis techniques for cross-sectional and longitudinal studies in osteoarthritis (OA) patients.[3]

There are a number of pulse sequence used in human medicine that have been found to yield the most accurate results for measuring cartilage thickness. A common sequence used for morphological imaging of cartilage is a three dimensional spoiled gradient echo sequence with fat suppression (3D SPGR-FS). [5,6]

Other MRI sequences have been also been investigated. A 2006 publication[7] outlined several sequences which address two imaging problems:

1. Conventional sequences provide insufficient spatial resolution and inadequate data about cartilage physiology.
2. Long image acquisition times required for 3D-SPGR sequences require longer periods of patient general anesthesia and increased risk of image degradation secondary to motion artifacts.

This study suggested that DEFT (Driven Equilibrium Fourier Transformation), BSSFP (Balanced Steady State Free Precision) and fat water separation sequences allow good assessment of cartilage with acceptable spatial resolution and decreased acquisition times [7].

A 2008 study evaluated cartilage thickness and volume changes over time in dogs as a model for OA in humans.[18] This study was conducted on five dogs that had surgical transection of their cranial cruciate ligaments. Serial MRI studies of the stifle were then carried out post immediately and at 4, 8 and 26 weeks post cranial cruciate ligament transection. The dogs were euthanized at 26 weeks and the joint cartilage was evaluated grossly for defects. This study reported a general loss of cartilage thickness throughout the time period of the study. Cartilage loss was most pronounced on the tibial plateau. The paper reported good correlation between gross cartilage observations and cartilage volume changes ($r = -0.81$ $p < 0.001$) although there was no reported assessment of accuracy of MRI at evaluating cartilage thickness compared to histology measurements.

A 2011 study evaluated cartilage volume changes in the canine stifle over time after cranial cruciate ligament transection and extracapsular surgical stabilization[19]. Thirty one dogs had surgical transection of the cranial cruciate ligament. After 4 weeks, surgical extracapsular stabilization was performed and the dogs were divided into 2 treatment groups for the purpose of evaluating if tiludronic acid was able to decrease the progression of OA. MRI examination of the stifle joints was carried out at 10, 26,91, 210 and 357 days post cranial cruciate ligament transection. This study reported an initial decrease in cartilage volume post cranial cruciate ligament transection which stabilized after extracapsular stabilization. The dogs were euthanized on day 364 and cartilage was examined grossly. This study did not evaluate the accuracy of MRI at evaluating cartilage thickness.

To the author's knowledge, although studies have been performed to assess cartilage volume change over time,[18,19] no studies have been carried out to evaluate the ability of MRI to accurately and precisely measure cartilage thickness in dogs. The Auburn University College of Veterinary Medicine currently has an MRI unit with sufficient field strength (1.5T) to obtain images using pulse sequences used in human and veterinary medicine to evaluate cartilage thickness and morphology.

III. MATERIALS AND METHODS

Animal Subjects

Eleven normal pelvic limbs were disarticulated at the level of the coxofemoral joint from 6 cadaver dogs of various breeds, age and gender, with a body weight >15kg. Using power analysis, a population of eleven dogs with a proposed correlation of 0.8 yielded an acceptable power of >0.9. The dogs were previously enrolled in a separate IAACUC approved study at Auburn University College of Veterinary Medicine. The limbs were obtained within 1 hour of euthanasia and immediately refrigerated at approximately $+4^0$C. Image acquisition occurred within 48hrs of euthanasia. Each limb was radiographed to evaluate for evidence of gross joint abnormalities that would necessitate exclusion from the study (e.g. neoplastic disease within the joint or presence of a metallic bone plate).

Magnetic Resonance Imaging

Each stifle was imaged in extension with the caudal surface in contact with the table. Each stifle joint was placed at the isocenter of a 1.5T MRI unit (Philips Medical Systems, Milwaukee) in a human extremity coil (Quadrature Lower Extremity, Philips Medical Systems, Milwaukee, WI, Model 473P1-64H, Frequency 63.73 MHz). Three separate image sequences were acquired in the sagittal plane through each stifle (Figure 1):

1. Proton Density Spin Echo (PDSE) (slice thickness 2mm, gap 0mm, time to echo (TE) 7.7ms, repetition time (TR) 150.0ms, flip angle 90^0, number of acquisitions 2, field of view 220mm, matrix 384 × 512, pixel size 0.57 × 0.69mm)

2. 3 dimensional spoiled gradient fat suppression (3D SPGR-FS), (slice thickness 2mm, gap 0mm, time to echo (TE) 7.0ms, repetition time (TR) 42.0ms, flip angle 20^0, number of acquisitions 2, field of view 220mm, matrix 384 × 512, pixel size 0.57 × 0.69mm).
3. Steady State Free Precision (SSFP) (slice thickness 2mm, gap 0mm, time to echo (TE) 8.0ms, repetition time (TR) 500.0ms, flip angle 90^0, number of acquisitions 2, field of view 220mm, matrix 384 × 512, pixel size 0.57 × 0.69mm).

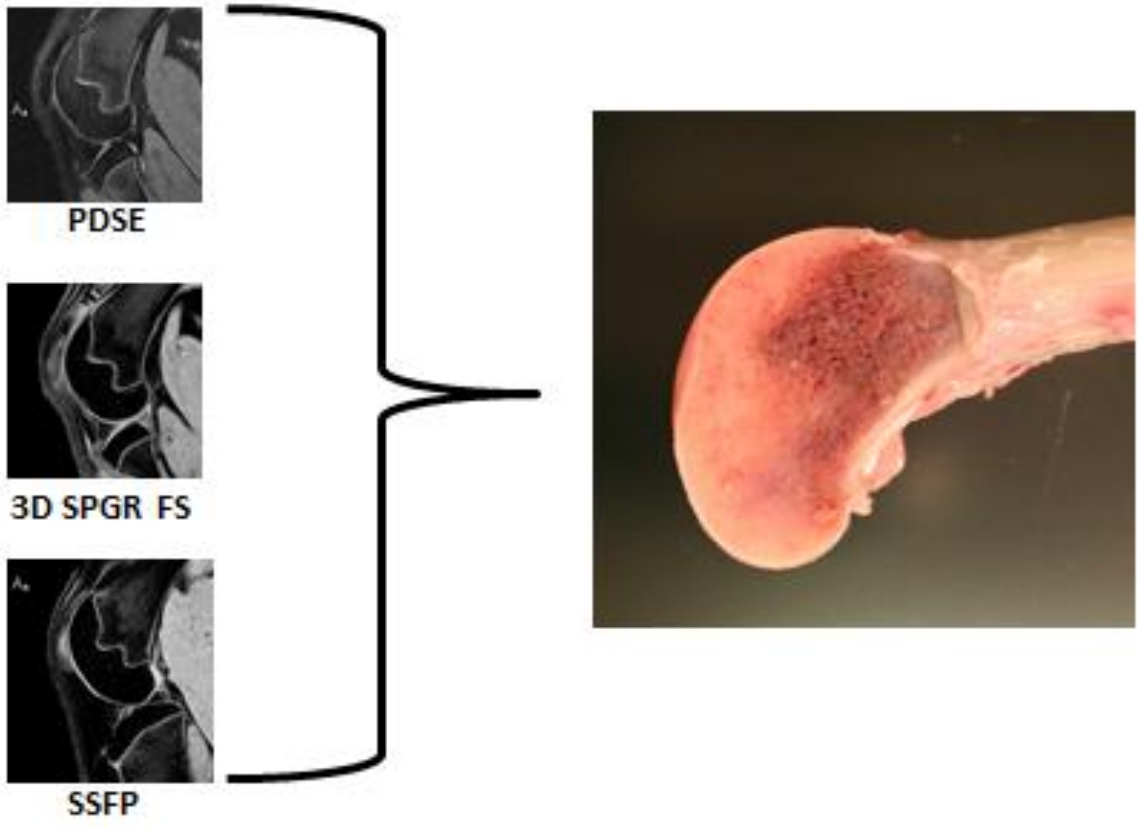

Figure 1. Left: PDSE, 3D SPGR FS and SSFP MRI sequences were obtained of the stifles in a sagittal plane. Right: Femoral condyles were sectioned in the sagittal plane.

Image Analysis

Images were analyzed at a diagnostic workstation by the author (LB) together with two board certified veterinary radiologists (MH, JTH) independently. Cartilage thickness was measured using the Osirix DICOM viewer software measuring tool. Measurements of cartilage thickness were made at the mid-sagittal point of the medial and lateral femoral condyles. The reason for measuring cartilage thickness at these specific sites was because their spatial location was easy to identify and section during preparation of histological samples. Cartilage was identified as a layer of increased signal intensity located between the subchondral bone which emitted no radiofrequency signal and the synovial fluid which had low signal intensity (Figure 2) as suggested by Olive et al. (2010) in a previous study.[20] Measurements were made perpendicular to the bone surface. Three measurements were made at each site and an average value calculated. Repeatability of MRI measurements were determined using standard deviation and a repeatability index based on replications and the residual error. The repeatability index was calculated by subtracting the measurement error percentage from 100%.

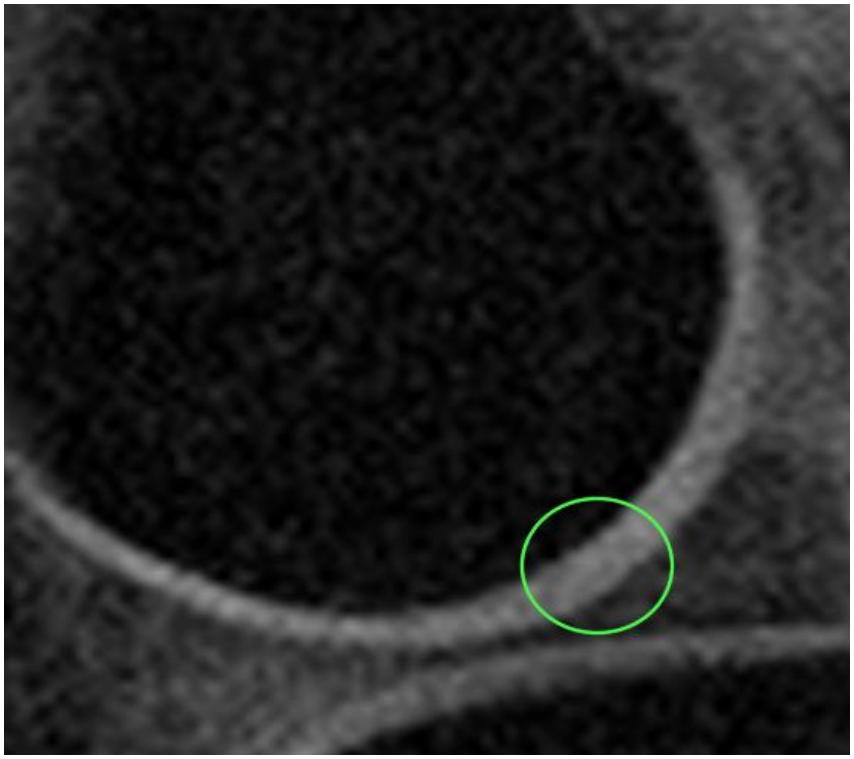

Figure 2. Cartilage was identified as a layer of increased signal intensity between the subchondral bone which emitted no radiofrequency signal and the synovial fluid which had low signal intensity.

Histology Sampling

The stifle joints were then prepared for gross cartilage thickness evaluation. After magnetic resonance imaging was completed, the stifles were refrigerated at approximately $+4^0$C with histologic preparation beginning within 48 hours to minimize post mortem changes to cartilage which could affect thickness. Histologic samples were taken from the approximate sites analyzed with MRI. Sample preparation was carried out by the primary investigator after training and supervision from a board certified pathologist (CJ). Four-millimeter-thick osteochondral slices were made through the medial and lateral condyles in a sagittal plane (Figure 3). Samples of bone were histologically processed as described in previous studies[8,9].

Slices were fixed in 10% buffered formaldehyde (pH 7.4) for 48 hours and then decalcified in a Decalcifier II™ (Surgipath Medical Industries, Inc., Richmond, IL). The samples were processed routinely for histology, embedded in paraffin, and sectioned at 5μm thickness, followed by staining with hematoxylin and eosin (H&E) and toluidine blue to distinguish cartilage and bone (Figure 4).

Figure 3. Gross sagittal sections were cut through each femoral condyle.

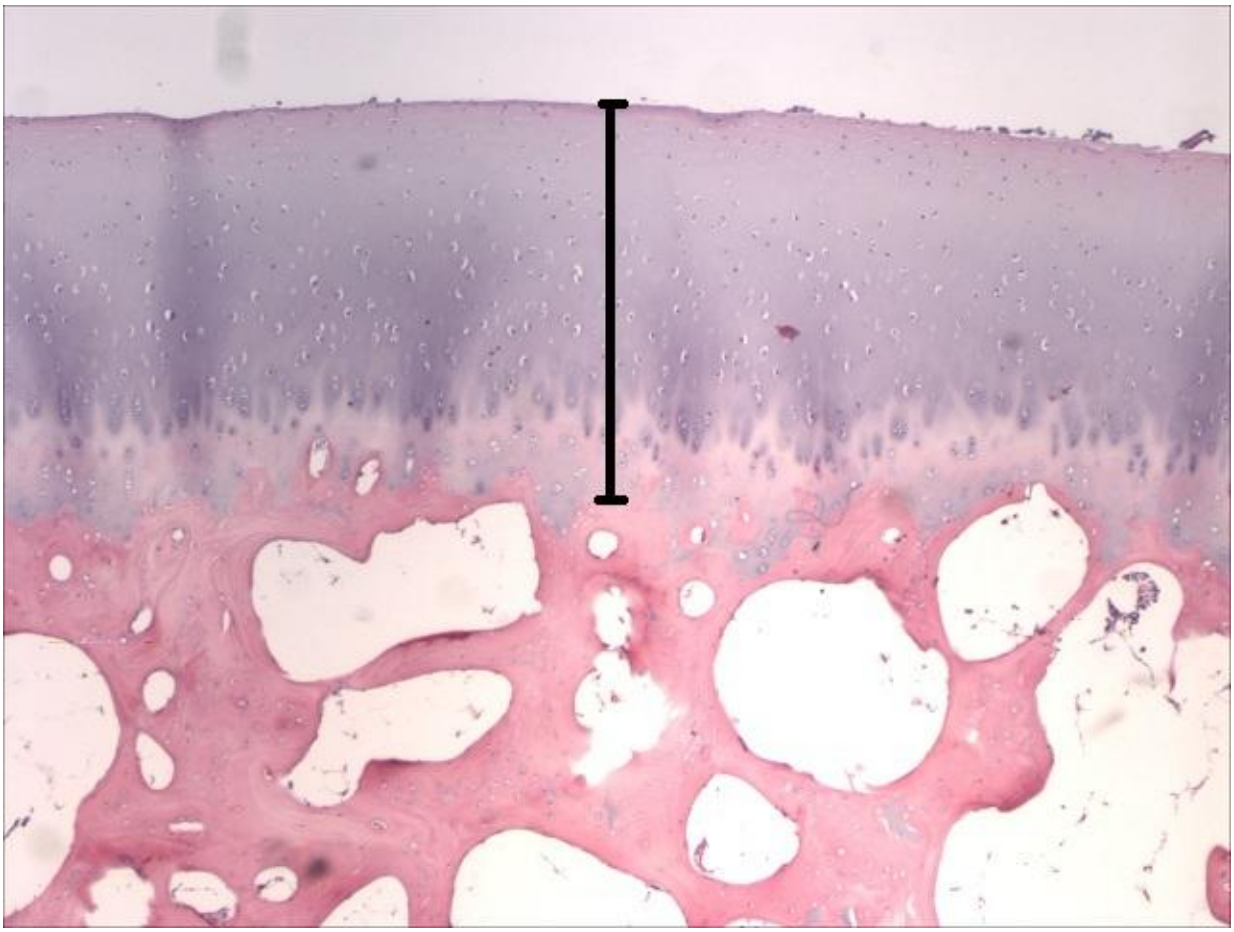

Figure 4. Histologic section of the articular cartilage of a femoral condyle stained with hematoxylin and eosin (H&E) and toluidine blue to distinguish cartilage and bone. **Cartilage thickness measurements, as shown, included the calcified zone.**

The samples were then examined by light microscopy and images of cartilage were captured (Q-Capture software, Q-Imaging Corp, Burnaby, BC, Canada) and cartilage thickness measured by digital morphometry (Image J, National Institutes of Health, Bethesda, Maryland, USA). These measurements were carried out by the primary investigator with guidance and training from a board certified veterinary pathologist (CJ). Ten independent measurements were

conducted for each specimen and expressed as the median and interquartile range. Data from each group was compared using a two-tailed Mann-Whitney *U* test.

Statistical Analysis

Data was entered into a spreadsheet using Microsoft Excel 2010 and analyzed using Statistical Analysis System software (SAS, release version 9.2, Carey N.C.) The values for mean cartilage thickness from MRI and histology were compared using regression, correlation, and student's t test. Pearson's Correlation was used to assess correlation of cartilage thickness values obtained from magnetic resonance images and histology as well as to assess correlation among readers.

IV. RESULTS

MRI images of all eleven stifles using all three of the image sequences (PDSE, 3D SPGR-FS, SSFP) were obtained in the sagittal plane. All images were subjectively assessed as having sufficient signal to noise ratio (SNR) for image analysis. All images had hyperintense signal in the region of the articular cartilage of the femoral condyles. A total of 66 magnetic resonance images were obtained for analysis by the three readers (LB, JTH, MH).

Acceptable histological samples were obtained from all condyles of all stifles. Five condyles (B1med, B2 lat, C2 lat, D2 med and F1 lat) were re-sectioned from the samples obtained due to folding artifact on the initial slides.

Values for the paired student t test using pooled measurements of the readers showed significant differences between the mean cartilage thickness measured from histologic section and the MRI thicknesses for all sequences ($p < 0.05$). For individual readers, there was no significant difference in 14/66 images (reader 1), 25/66 images (reader 2) and 1/66 images (reader 3) when comparing the mean cartilage thickness measurements between histology and MR ($p>0.05$). Of the 40 images for all readers with no significant difference between the cartilage thickness measured by histology and MRI, 16 were SSFP images, 12 PDSE and 4 3D SPGR-FS images ($p>0.05$).

The mean cartilage thickness values for all three MRI sequences pooled for all readers were greater than the mean value obtained from the histological measurements (See figures 5-7).

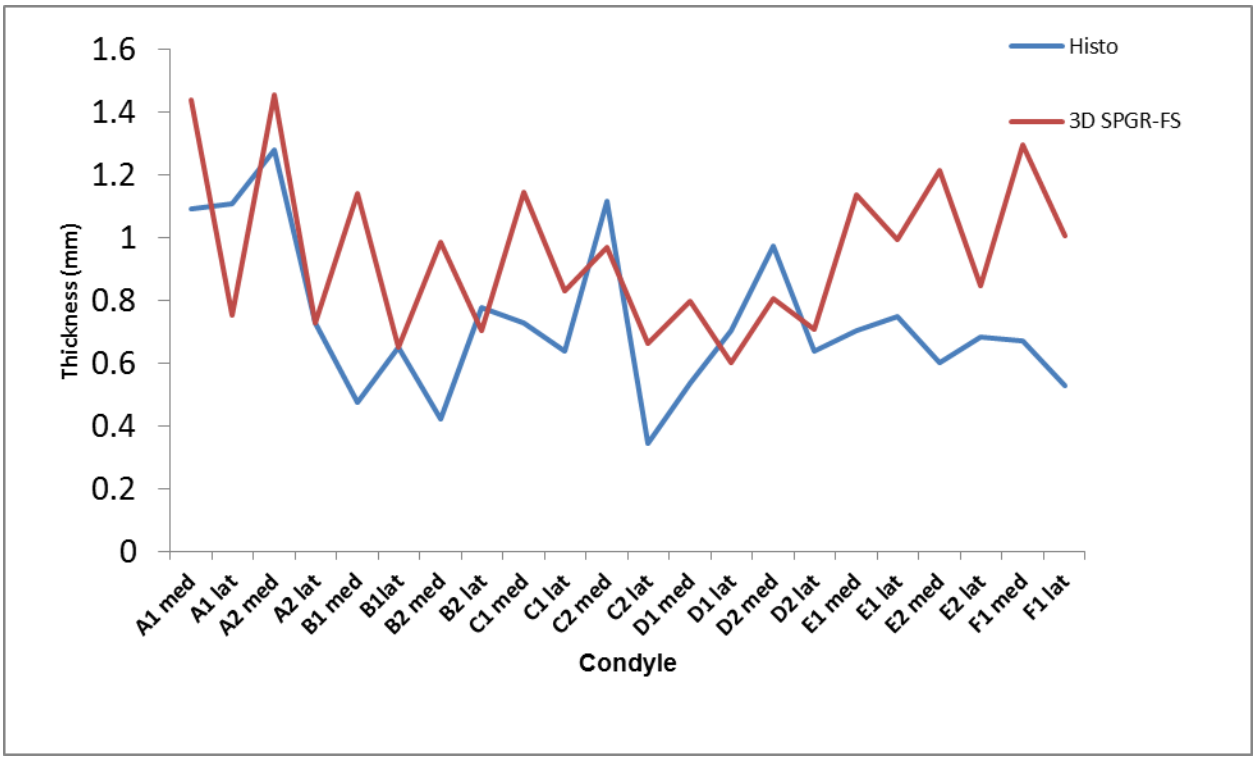

Figure 5. Measurements (mm) from the femoral condyle made using histology and a 3D SPGR-FS MRI imaging sequence. The mean cartilage thickness measured using 3D SPGR-FS images was 0.949mm compared to a mean histological measurement of 0.734mm.

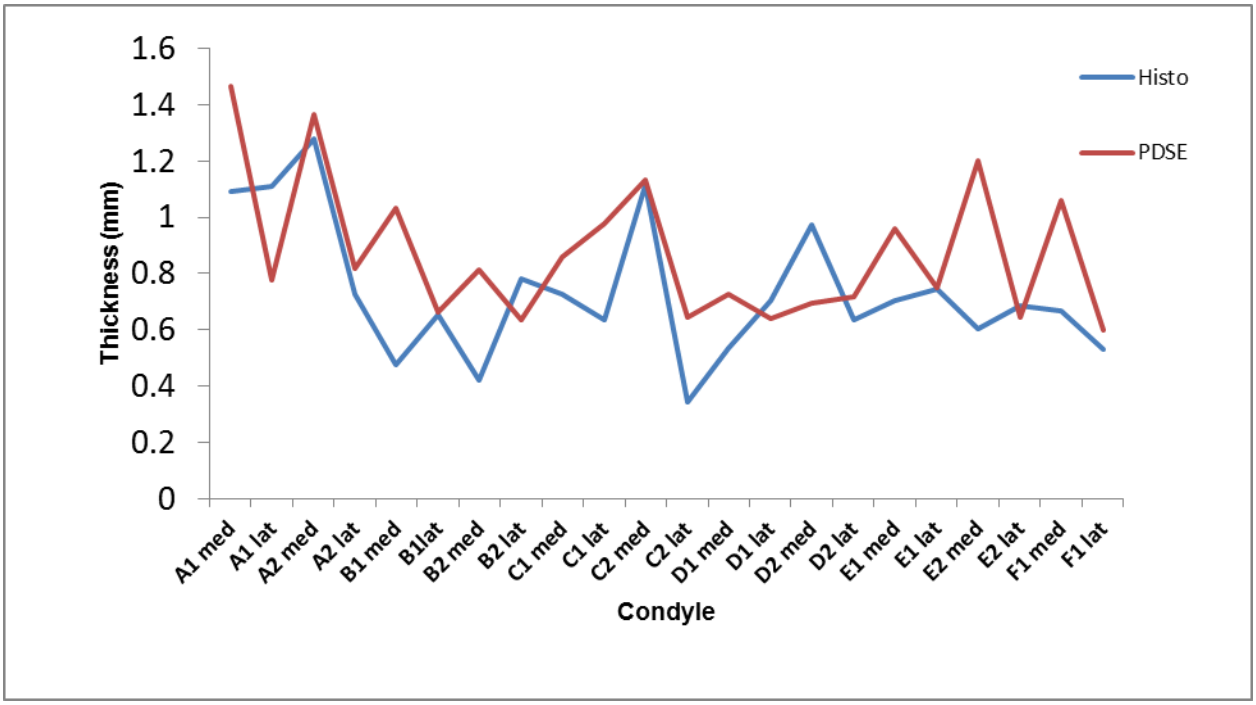

Figure 6. Measurements (mm) from the femoral condyle made using histology and a PDSE MRI sequence. The mean cartilage thickness measured using PDSE images was 0.872mm compared to a mean histological measurement of 0.734mm.

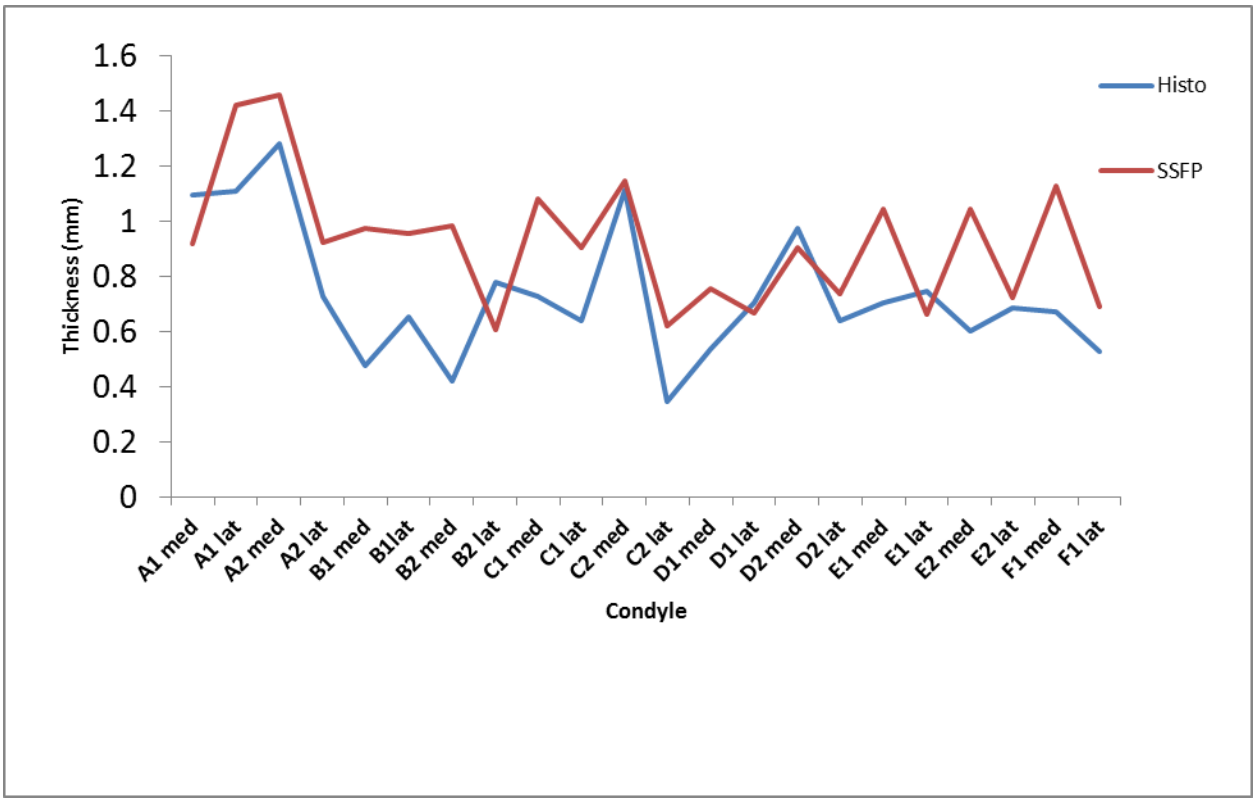

Figure 7. Measurements (mm) from the femoral condyle made using histology and an SSFP MRI imaging sequence. The mean cartilage thickness measured using SSFP images was 0.924mm compared to a mean histological measurement of 0.734mm.

Pearsons rank correlation coefficient values, that were statistically significant ($p<0.05$), showed poor to moderate correlation between histology measurements and MRI images for all readers (R values: 0.25 to 0.77) (appendix I). Good correlation ($R>0.78$ ($p<0.05$)) between readers was present for 3D SPGR-FS images of medial condyles; between readers 1 and 2 for SSFP images of medial condyles and for all readers for SSFP images of the lateral condyle. There was poor to moderate correlation between readers for all MRI images of the other condyles. Moderate correlation was present between readers 1 and 2 for 3D SPGR-FS images of

the lateral condyles; between readers 1 and 3 for PD images of the lateral condyles and between all readers for PD images of the medial condyle. All other R values between readers were not statistically significant.

Regression of all three MRI sequence images showed a poor coefficient of variation (R^2: 0.40). Regression for individual sequences compared to histology showed poor coefficient of variations for all image types (3D SPGR-FS: 0.11, PDSE: 0.25 and SSFP: 0.35) (appendix II) with SSFP having the highest value.

V. DISCUSSION

MRI has revolutionized musculoskeletal imaging in human medicine with its ability to differentiate cartilage and periarticular soft tissue structures because of increased contrast resolution compared to other modalities. There continues to be substantial research assessing and improving quantitative evaluation of cartilage as cartilage thickness may prove to be a powerful marker for osteoarthritis (OA).[11] Non-invasive evaluation of cartilage thickness has potential in veterinary medicine to objectively assess progression of articular disease as well as response to drug and neutraceutical therapy over time. This modality therefore represents a useful tool in quantitative evaluation of the canine stifle joint.

To the author's knowledge, this is the first study in veterinary medicine that has investigated the efficacy of MRI to quantitatively evaluate cartilage thickness in small animals. A recent study by Olive et al. evaluated the ability of 3D SPGR-FS images for evaluating cartilage thickness and detecting full thickness denuration in the metacarpophalangeal joint in horses[1]. Olive et al. reported moderate correlation (0.44 $p<0.0001$) between MR thickness measured with 3D SPGR-FS images (0.90mm ± 0.17mm) and histology (0.79mm ± 0.16mm)[1]. The results from this study differ from Olive et al. showing poor correlation between 3D SPGR-FS images and histology with R values ranging from -0.26 to 0.41 for all readers. Olive et al reported 3D SPGR-FS images significantly overestimated cartilage thickness <1mm in thickness, which is consistent with the results from this current study.

Correlation of MRI measurements for all sequences between readers was variable. The highest significant correlation ($p<0.05$) between most readers was with SSFP images of the lateral condyle suggesting that this sequence is the most precise of the three sequences for evaluating cartilage thickness. The coefficient of variation between the MRI images and

histology measurement was highest for SSFP images (0.30) suggesting this sequence to be the most accurate of the sequences for evaluating cartilage thickness, however; this value is considered low.

Study limitations

There are several factors in the study design which may have contributed to error between MRI and histological measurements of cartilage thickness:

Images were obtained on cadaver specimens. To minimize potential post mortem changes on image quality and variability, MRI images were obtained within 48 hours after euthanasia. A study by Bolen et al. (2010) studied how refrigerating equine cadaver limbs at 4 ^{0}C would affect the subjective quality and signal changes of various anatomic structures for magnetic resonance imaging. Bolen et al. reported no subjective change in image quality, and there was no reported changes in cartilage signal. The author believes that the changes from refrigeration in the current study were likely minimal, however; future study design could include image acquisition prior to euthanasia to avoid influence from refrigeration.

The parameters used during the acquisition of the MRI images for all sequences contribute to the signal to noise ratio (SNR) and spatial resolution, which are inherent in the MRI sequence properties. The aim of sequence design and planning is to gain maximal spatial resolution with acceptable SNR for image interpretation. Volume averaging associated with voxel dimension of the MRI images is a function of the image field of view (FOV) and matrix size.[12] The smallest voxel size achievable is most desirable, but results in decreased SNR of the image. A small image FOV is desirable to minimize the voxel size but this in turn increases the risk of aliasing artifacts creating unacceptable anatomic representation. In this study, FOV and

matrix size were standardized for all stifles with the stifle orientated as if a patient was in dorsal recumbency. In a clinical setting FOV and matrix size may have to be varied depending on the size of the leg and individual positioning needs of the patient.

SNR of a MRI image is influenced by magnetic field strength by a factor of B^1 to $B^{1.5}$ where B represents the factor of increase in magnetic field strength.[12] This means an increase in the field strength of the magnet from 0.5T to 1.5T would result in an increase in SNR from 3-5 times. The field strength of the magnet in this study was 1.5T, a common high field strength magnet at many academic referral veterinary institutions. Higher strength magnets are becoming available for clinical use (e.g. 3T) and research (e.g. 7T). These units potentially will improve SNR and allow smaller voxel sizes to be used; however, T1 relaxation times increase with higher field strength resulting in longer image acquisition times. Longer image acquisition times translate to increased artifact production and increased saturation of short T1 tissues which in turn lead to decreased contrast sensitivity.[12] Future studies with higher strength magnets must therefore consider these other factors to optimize image quality and practicality for acquisition with clinical patients. A study by Pepin et al. (2009)[22] used a 3D SPGR MRI sequence with a 7T magnet. The total imaging time for one stifle in the coronal plane using a 7T was 15 minutes[22] compared with approximately 8 minutes for this study using a 1.5T magnet.

There was likely error associated with the decalcification procedure and histological processing of the condyle specimens. To the author's knowledge, no study has been performed investigating the alteration of cartilage thickness in vivo versus ex vivo and the effect of decalcification prior to processing with a microtome. Cano-Sánchez et al. (2005) describe a procedure for slide preparation of bone samples which does not involve decalcification. They describe a cutting and grinding technique known as the EXAKT system (EXAKT Vetriebs,

Norderstedt, Germany). This technique is used to minimize sample shrinkage by not using a decalcification procedure and may be a suitable alternative study design. However, the equipment is expensive, not readily available and utilizes dehydration techniques which may still alter cartilage thickness.

The stifle joint is a complex condylar synovial joint with rounded condyles[14]. Because of the conformation of the condyle, there is error associated with angle variation of the sagittal plane through the femur constructed during the MRI image acquisition and slice angle through the femur during preparation of the histological samples. Therefore, there is potential artificial cartilage thickening on a histological section or MRI image if the plane of cut is <90° from the subchondral bone surface. There is also error from the accuracy of correlating the MRI image and histological slice locations.

All three readers differ in their amount of career experience reading musculoskeletal MR images although MRI is a relatively new modality. Reader 1 was a 2nd year radiology resident and readers 2 and 3 were ACVR board certified radiologists. It may have been interesting to include readers with different levels of experience reading MRI images (e.g. radiologists, orthopedic surgeons and residents) and compare the differences between readers.

The project did not aim to address variation in cartilage thickness between legs or between patients. The primary concern was to compare the ability of the different MRI sequences in their ability to assess cartilage thickness. Olive et al.[1] evaluated the ability of 3D SPGR-FS sequence images at identifying full thickness cartilage denurations with moderate sensitivity (0.56) and high specificity (0.92). However, these lesions were artificially introduced post mortem to the articular cartilage of equine metacarpophalangeal joints. Identifying full thickness denuration in the canine stifle in a similar study may also be worthwhile. Although in vivo cartilage loss

results in subchondral bone changes and has been studied in human medicine,[11,15] fewer studies have been performed in veterinary medicine.[16,17] Identification of full thickness lesions in clinical cases may be more relevant but study design may be difficult.

VI. CONCLUSION

This study was designed to evaluate the ability of MRI to accurately represent cartilage thickness in the canine stifle and to determine if there was a difference in measurements between the sequences. The majority of MRI cartilage thickness measurements were statistically different from those measured by histology and so objectively the null hypothesis that measurements of cartilage thickness in dogs using MRI are identical to measurements taken using histopathology can be rejected. However, subjectively the MRI sequences investigated were able to clearly represent articular cartilage of the canine stifle and further studies with a larger number of samples and higher field strength magnets may be able to more accurately depict cartilage thickness. As BSSFP sequences had the highest number of images that showed cartilage thickness to be significantly similar to histology measurements, further investigation into its use may be warranted for cartilage imaging in small animals

The good correlation between readers for MRI measurement using the 3DSPGR and BSSFP images for the medial and lateral condyles respectively suggest MRI may offer a precise tool for evaluating cartilage thickness and may warrant further investigation with a larger sample size.

REFERENCES

1. Olive J, d'Anjou MA, Girard C, et al. Fat-suppressed spoiled gradient-recalled imaging of equine metacarpophalangeal articular cartilage. Vet Radiol Ultrasound 2010; 51:107-115.
2. Ettinger SJ, Feldman EC. Textbook of Veterinary Internal Medicine. 6th Edition 2005. Elsevier Saunders. p. 83
3. Eckstein F, et al. Magnetic resonance imaging (MRI) of articular cartilage in knee osteoarthritis (OA): morphological assessment. Osteoarthritis Cartilage 2006;14:A46-A75.
4. Murray RC, Branch MV, et al. Validation of magnetic resonance imaging for measurement of equine articular cartilage and subchondral bone thickness. Am J Vet Res 2005;66:No11: 1999-2005
5. McCauley TR, Disler DG. Magnetic resonance imaging of articular cartilage of the knee. J Am Acad Orthop Surg 2001;9:2e8.
6. Disler DG. Fat-suppressed three-dimensional spoiled gradient recalled MR imaging: assessment of articular and physeal hyaline cartilage. AJR Am J Roentgenol 1997;169; 1117e23.
7. Gold GE, et al. MRI of articular cartilage in OA: novel pulse sequences and compositional/functional markers. Osteoarthritis and Cartilage 2006;14,A76eA86.
8. Ytrehus B, Ekman S, et al. Focal changes in blood supply during normal epiphyseal growth are central in the pathogenesis of osteochondrosis in pigs. Bone 2004;35(6): 1294-1306.
9. Olson EJ, Lindgren BR, et al. Effects of long-term estrogen replacement therapy on the prevalence and area of periarticular tibial osteophytes in surgically postmenopausal cynomolgus monkeys. Bone 2007; 41(2): 282-289.
10. Fossum TW, Hedlund CS, Hulse DA, Johnson AL, Seim III HB, Willard MD, Carroll GL. Small animal surgery. 2nd Edition. Mosby. p1024. 2002

11. Eckstein F, Worth, W. Quantitative cartilage imaging in knee osteoarthritis. Review Article. Arthritis 2011. Volume 2011, Article ID 475684. Hindawi Publishing Corporation. 19 pages.
12. Bushburg JT, Seibert JA, Leihdoldt EM Jr, Boone JM. The essential physics of medical imaging. 2nd Edition. 2002. Lippincott Williams & Wilkins. pp 439-442.
13. Cano-Sánchez J, Campo-Trapero J, Gonzalo-Lafuente JC, Moreno-López LA, Bascones-Martínez A. Undecalcified bone samples: a description of the technique and its utility based on the literature. Med Oral Patol Oral Cir Bucal 2005;10:E74-E87
14. Evans HE. Miller's Anatomy of the dog. 3rd Edition. 1993. Saunders. p246.
15. Jans LBO. MR imaging findings of lesion involving cartilage and bone in the paediatric knee: a pictorial review. Organe de la Société royale belge de radiologie. 2011;94:247-253
16. Martig S, Boisclair J, Konar M, et al: MRI characteristics and histology of bone marrow lesions in dogs with experimentally induced osteoarthritis. Vet Radiol Ultrasound 48:105–112, 2007
17. D'Anjou MA, Moreau M, Troncy E, Martel-Pelletier J, Abram F, Raynauld JP, Pelletier. Osteophytosis, subchondral bone sclerosis, joint effusion and soft tissue thickening in canine experimental stifle osteoarthritis: comparison between 1.5T magnetic resonance imaging and computed radiography. Vetsurg 2008;37:166-177
18. Boileau C, Martel-Pelletier J, Abram F, et al. Magnetic resonance imaging can accurately assess the long-term progression of knee structural changes in experimental dog osteoarthritis. Ann Rheum Dis. 2008; Jul;67(7):926-32
19. Pelletier JP, Troncy E, Bertaim T, Thibaud et al. Treatment with tiludronic acid helps reduce the development of experimental osteoarthritis lesions in dogs with anterior cruciate ligament transection followed by reconstructive surgery: a 1-year study with quantitative magnetic resonance imaging. J Rheumatol 2011; Jan;38(1):118-128
20. Olive J, D'Anjou MA, Alexander K, Laverty S, Theoret C. Comparison of magnetic resonance imaging, computed tomography, and radiography for assessment of non-cartilagenous changes in equine metacarpophalangeal osteoarthritis. Vet Radiol Ultrasound 51: 267-279, 2010

21. Bolan G, Haye D, Dondelinger R, Busoni V.Magnetic resonance signal changes during time in equine limbs refrigerated at 4^0C. Vet Radiol Ultrasound 51: 19-24, 2010
22. Pepin SR, Griffith CJ, Wijdicks CA, et al. A comparative analysis of 7.0-tesla magnetic resonance imaging and histology measurements of knee articular cartilage in a canine posterolateral knee injury model. The American Journal of Sports Medicine 37: S1 pp 119S-124S

APPENDICES

APPENDIX I

Pearson's Correlation Coefficients

---------- image=3DSFPG condyle=lat ----------

The CORR Procedure

4 Variables: brown_ holland hathcock histo

Simple Statistics

Variable	N	Mean	Std Dev	Sum	Minimum	Maximum	Label
brown_	11	0.86215	0.15958	9.48367	0.63967	1.11000	brown
holland	11	0.69739	0.18878	7.67133	0.37467	0.99767	holland
hathcock	11	0.75506	0.15848	8.30567	0.59033	1.02600	hathcock
histo	11	0.68664	0.18476	7.55303	0.34494	1.11027	histo

Pearson Correlation Coefficients, N = 11
Prob > |r| under H0: Rho=0

	brown_	holland	hathcock	histo
brown_	1.00000	0.61478	0.42353	0.18106
brown		0.0441	0.1943	0.5942
holland	0.61478	1.00000	0.29085	0.05462
holland	0.0441		0.3856	0.8733
hathcock	0.42353	0.29085	1.00000	-0.25671
hathcock	0.1943	0.3856		0.4461
histo	0.18106	0.05462	-0.25671	1.00000
histo	0.5942	0.8733	0.4461	

---------- image=3DSFPG condyle=med ----------

The CORR Procedure

4 Variables: brown_ holland hathcock histo

Simple Statistics

Variable	N	Mean	Std Dev	Sum	Minimum	Maximum	Label
brown_	11	1.20718	0.21197	13.27900	0.87367	1.54667	brown
holland	11	1.20118	0.25355	13.21300	0.80467	1.62000	holland
hathcock	11	0.97030	0.24031	10.67333	0.61300	1.29667	hathcock
histo	11	0.78150	0.28835	8.59649	0.42233	1.28036	histo

Pearson Correlation Coefficients, N = 11
Prob > |r| under H0: Rho=0

	brown_	holland	hathcock	histo
brown_	1.00000	0.94933	0.81998	0.41438
brown		<.0001	0.0020	0.2051
holland	0.94933	1.00000	0.78038	0.37582
holland	<.0001		0.0046	0.2547
hathcock	0.81998	0.78038	1.00000	0.26325
hathcock	0.0020	0.0046		0.4341
histo	0.41438	0.37582	0.26325	1.00000
histo	0.2051	0.2547	0.4341	

---------- image=PD condyle=lat ----------

The CORR Procedure

4 Variables: brown_ holland hathcock histo

Simple Statistics

Variable	N	Mean	Std Dev	Sum	Minimum	Maximum	Label
brown_	11	0.78036	0.10679	8.58400	0.60367	0.95400	brown
holland	11	0.75976	0.16758	8.35733	0.55600	1.18000	holland
hathcock	11	0.60676	0.09887	6.67433	0.45767	0.80133	hathcock
histo	11	0.68664	0.18476	7.55303	0.34494	1.11027	histo

Pearson Correlation Coefficients, N = 11
Prob > |r| under H0: Rho=0

	brown_	holland	hathcock	histo
brown_	1.00000	0.74928	0.68614	0.32598
brown		0.0079	0.0197	0.3279
holland	0.74928	1.00000	0.57513	-0.02502
holland	0.0079		0.0642	0.9418
hathcock	0.68614	0.57513	1.00000	0.59433
hathcock	0.0197	0.0642		0.0538
histo	0.32598	-0.02502	0.59433	1.00000
histo	0.3279	0.9418	0.0538	

------------------------------------ image=PD condyle=med ------------------------------------

The CORR Procedure

4 Variables: brown_ holland hathcock histo

Simple Statistics

Variable	N	Mean	Std Dev	Sum	Minimum	Maximum	Label
brown_	11	1.15942	0.28529	12.75367	0.72867	1.56667	brown
holland	11	1.13503	0.28110	12.48534	0.81400	1.76667	holland
hathcock	11	0.82724	0.28092	9.09967	0.47700	1.29667	hathcock
histo	11	0.78150	0.28835	8.59649	0.42233	1.28036	histo

Pearson Correlation Coefficients, N = 11
Prob > |r| under H0: Rho=0

	brown_	holland	hathcock	histo
brown_	1.00000	0.74983	0.63039	0.25234
brown		0.0079	0.0376	0.4541
holland	0.74983	1.00000	0.77649	0.54952
holland	0.0079		0.0049	0.0799
hathcock	0.63039	0.77649	1.00000	0.54284
hathcock	0.0376	0.0049		0.0844
histo	0.25234	0.54952	0.54284	1.00000
histo	0.4541	0.0799	0.0844	

---------- image=SSFP condyle=lat ----------

The CORR Procedure

4 Variables: brown_ holland hathcock histo

Simple Statistics

Variable	N	Mean	Std Dev	Sum	Minimum	Maximum	Label
brown_	11	0.90991	0.26843	10.00900	0.64233	1.55000	brown
holland	11	0.79976	0.21872	8.79733	0.56067	1.37667	holland
hathcock	11	0.71812	0.23625	7.89933	0.49433	1.32667	hathcock
histo	11	0.68664	0.18476	7.55303	0.34494	1.11027	histo

Pearson Correlation Coefficients, N = 11
Prob > |r| under H0: Rho=0

	brown_	holland	hathcock	histo
brown_	1.00000	0.90742	0.97967	0.64690
brown		0.0001	<.0001	0.0315
holland	0.90742	1.00000	0.93626	0.77078
holland	0.0001		<.0001	0.0055
hathcock	0.97967	0.93626	1.00000	0.68314
hathcock	<.0001	<.0001		0.0205
histo	0.64690	0.77078	0.68314	1.00000
histo	0.0315	0.0055	0.0205	

---------- image=SSFP condyle=med ----------

The CORR Procedure

4 Variables: brown_ holland hathcock histo

Simple Statistics

Variable	N	Mean	Std Dev	Sum	Minimum	Maximum	Label
brown_	11	1.09042	0.19315	11.99467	0.85033	1.58667	brown
holland	11	1.10315	0.18790	12.13467	0.76100	1.51667	holland
hathcock	11	0.99852	0.34277	10.98367	0.65567	1.86333	hathcock
histo	11	0.78150	0.28835	8.59649	0.42233	1.28036	histo

Pearson Correlation Coefficients, N = 11
Prob > |r| under H0: Rho=0

	brown_	holland	hathcock	histo
brown_	1.00000	0.89773	0.35565	0.46196
brown		0.0002	0.2831	0.1526
holland	0.89773	1.00000	0.54722	0.54504
holland	0.0002		0.0815	0.0829
hathcock	0.35565	0.54722	1.00000	0.23767
hathcock	0.2831	0.0815		0.4816
histo	0.46196	0.54504	0.23767	1.00000
histo	0.1526	0.0829	0.4816	

APPENDIX II

Analysis of Variance data and Regression

The SAS System 16:20 Monday, March 5, 2012 1

Obs	code	Condyle	Histo	PD	_DFSSPGR	SSFP
1	A1 med	med	1.09273	1.46778	1.43778	0.91611
2	A1 lat	lat	1.11027	0.77478	0.75167	1.41778
3	A2 med	med	1.28036	1.36333	1.45667	1.45889
4	A2 lat	lat	0.72737	0.81722	0.72844	0.92167
5	B1 med	med	0.47445	1.03156	1.14122	0.97189
6	B1lat	lat	0.65208	0.66456	0.64933	0.95389
7	B2 med	med	0.42233	0.81133	0.98656	0.98200
8	B2 lat	lat	0.77945	0.63722	0.70544	0.60789
9	C1 med	med	0.72771	0.86056	1.14533	1.08200
10	C1 lat	lat	0.63769	0.97844	0.83033	0.90567
11	C2 med	med	1.11507	1.13500	0.96856	1.14522
12	C2 lat	lat	0.34494	0.64344	0.66189	0.61956
13	D1 med	med	0.53672	0.72600	0.79789	0.75567
14	D1 lat	lat	0.70375	0.63978	0.60322	0.66567
15	D2 med	med	0.97412	0.69500	0.80667	0.90178
16	D2 lat	lat	0.63706	0.71600	0.70933	0.73444
17	E1 med	med	0.70214	0.95856	1.13889	1.04100
18	E1 lat	lat	0.74723	0.75144	0.99578	0.66211
19	E2 med	med	0.60150	1.20111	1.21444	1.04311
20	E2 lat	lat	0.68417	0.64667	0.84500	0.72344
21	F1 med	med	0.66937	1.05933	1.29444	1.12756
22	F1 lat	lat	0.52903	0.59844	1.00644	0.68978

The SAS System 16:20 Monday, March 5, 2012 2

The REG Procedure
Model: MODEL1
Dependent Variable: Histo Histo

Number of Observations Read 22
Number of Observations Used 22

Analysis of Variance

Source	DF	Sum of Squares	Mean Square	F Value	Pr > F
Model	3	0.49919	0.16640	4.14	0.0214
Error	18	0.72312	0.04017		
Corrected Total	21	1.22231			

Root MSE	0.20043	R-Square	0.4084
Dependent Mean	0.73407	Adj R-Sq	0.3098
Coeff Var	27.30443		

Parameter Estimates

Variable	Label	DF	Parameter Estimate	Standard Error	t Value	Pr > |t|
Intercept	Intercept	1	0.17329	0.19651	0.88	0.3895
PD	PD	1	0.45921	0.34726	1.32	0.2026
_DFSSPGR	3DFSSPGR	1	-0.29328	0.31189	-0.94	0.3595
SSFP	SSFP	1	0.47488	0.23480	2.02	0.0582

The REG Procedure
Model: MODEL1
Dependent Variable: Histo Histo

Number of Observations Read 22
Number of Observations Used 22

Analysis of Variance

Source	DF	Sum of Squares	Mean Square	F Value	Pr > F
Model	1	0.30203	0.30203	6.56	0.0186
Error	20	0.92028	0.04601		
Corrected Total	21	1.22231			

Root MSE	0.21451	R-Square	0.2471
Dependent Mean	0.73407	Adj R-Sq	0.2095
Coeff Var	29.22194		

Parameter Estimates

Variable	Label	DF	Parameter Estimate	Standard Error	t Value	Pr > |t|
Intercept	Intercept	1	0.31243	0.17081	1.83	0.0823
PD	PD	1	0.48370	0.18880	2.56	0.0186

The REG Procedure
Model: MODEL2
Dependent Variable: Histo Histo

Number of Observations Read 22
Number of Observations Used 22

Analysis of Variance

Source	DF	Sum of Squares	Mean Square	F Value	Pr > F
Model	1	0.12941	0.12941	2.37	0.1395
Error	20	1.09291	0.05465		
Corrected Total	21	1.22231			

Root MSE	0.23376	R-Square	0.1059
Dependent Mean	0.73407	Adj R-Sq	0.0612
Coeff Var	31.84487		

Parameter Estimates

Variable	Label	DF	Parameter Estimate	Standard Error	t Value	Pr > |t|
Intercept	Intercept	1	0.44238	0.19599	2.26	0.0353
_DFSSPGR	3DFSSPGR	1	0.30741	0.19976	1.54	0.1395

The REG Procedure
Model: MODEL3
Dependent Variable: Histo Histo

Number of Observations Read	22
Number of Observations Used	22

Analysis of Variance

Source	DF	Sum of Squares	Mean Square	F Value	Pr > F
Model	1	0.42843	0.42843	10.79	0.0037
Error	20	0.79388	0.03969		
Corrected Total	21	1.22231			

Root MSE	0.19923	R-Square	0.3505
Dependent Mean	0.73407	Adj R-Sq	0.3180
Coeff Var	27.14102		

Parameter Estimates

Variable	Label	DF	Parameter Estimate	Standard Error	t Value	Pr > |t|
Intercept	Intercept	1	0.17445	0.17556	0.99	0.3323
SSFP	SSFP	1	0.60568	0.18436	3.29	0.0037

APPENDIX III

Histology measurements and Student t test

A1 Lateral

Measurement	Thickness (Pixels)	Thickness (mm)
1	1248	1.066667
2	1353	1.15641
3	1236	1.05641
4	1356	1.158974
5	1119	0.95641
6	1362.003	1.164105
7	1329	1.135897
8	1368.053	1.169276
9	1218.015	1.041038
10	1368.082	1.169301
Mean	1299.016	1.11027
St Dev	87.66918	0.074931

A1 Medial

Measurement	Thickness (Pixels)	Thickness (mm)
1	1314.003	1.123079
2	1260.004	1.076926
3	1269	1.084615
4	1242	1.061538
5	1229.477	1.050835
6	1284.897	1.098203
7	1317.342	1.125933
8	1327.401	1.134531
9	1291.687	1.104006
10	1281.594	1.095379
Mean	1278.496	1.092732
St Dev	29.9721	0.025617

Dr Brown
A1 Lateral

Measurement	PD (mm)	3DFSPG (mm)	SSFP (mm)
1	0.846	0.875	1.42
2	0.894	0.859	1.55
3	0.858	0.845	1.68
Mean	0.866	0.859666667	1.55
St Dev	0.024979992	0.015011107	0.13
T test	3.8166E-06	8.69454E-07	0.019738206
T test Pooled data	4.57267E-06	6.30856E-07	0.000214791

Dr Brown
A1 Medial

Measurement	PD (mm)	3DFSPG (mm)	SSFP (mm)
1	1.32	1.38	0.914
2	1.4	1.59	0.916
3	1.3	1.51	0.924
Mean	1.34	1.493333333	0.918
St Dev	0.052915026	0.105987421	0.005291503
T test	0.010380479	0.021045291	1.42846E-09
T test Pooled data	0.000119871	0.00075266	0.001584916

Dr Holland
A1 Lateral

Measurement	PD (mm)	3DFSPG (mm)	SSFP (mm)
1	0.7	0.594	1.37
2	0.712	0.599	1.4
3	0.709	0.623	1.36
Mean	0.707	0.605333333	1.376666667
St Dev	0.006245	0.015502688	0.02081666
T test	2.09E-08	6.16883E-10	5.66803E-07

Dr Holland
A1 Medial

Measurement	PD (mm)	3DFSPG (mm)	SSFP (mm)
1	1.19	1.52	0.973
2	1.16	1.53	0.941
3	1.18	1.52	0.952
Mean	1.176667	1.523333333	0.955333333
St Dev	0.015275	0.005773503	0.016258331
T test	0.000447	1.10085E-13	3.54713E-05

Dr Hathcock
A1 Lateral

Measurement	PD (mm)	3DFSPG (mm)	SSFP (mm)
1	0.812	0.824	1.35
2	0.751	0.815	1.27
3	0.691	0.731	1.36
Mean	0.751333	0.79	1.326667
St Dev	0.060501	0.051293	0.049329
T test	0.001085	0.000469	0.001849

Dr Hathcock
Medial

Measurement	PD (mm)	3DFSPG (mm)	SSFP (mm)
1	1.23	1.26	0.911
2	1.32	1.36	0.981
3	1.34	1.27	0.733
Mean	1.296667	1.296667	0.875
St Dev	0.058595	0.055076	0.127859
T test	0.021313	0.018038	0.094156

A2 Lateral

Measurement	Thickness (Pixels)	Thickness (mm)
1	887.788	0.758793
2	885.664	0.756978
3	972.801	0.831454
4	1000.931	0.855497
5	710.68	0.607419
6	714.146	0.610381
7	867.747	0.741664
8	888.324	0.759251
9	910.113	0.777874
10	825.66	0.705692
Mean	851.0253	0.727372
St Dev	106.7432	0.091234

A2 Medial

Measurement	Thickness (Pixels)	Thickness (mm)
1	1623.136	1.387296
2	1715.465	1.466209
3	1562.842	1.335762
4	1500.075	1.282115
5	1421.851	1.215257
6	1437.704	1.228807
7	1455.003	1.243592
8	1458	1.246154
9	1428.154	1.220644
10	1395.306	1.192569
Mean	1498.024	1.280362
St Dev	103.9515	0.088847

Dr Brown
A2 Lateral

Measurement	PD (mm)	3DFSPG (mm)	SSFP (mm)
1	0.893	0.974	1.09
2	0.92	0.935	1.06
3	0.907	1.04	1.12
Mean	0.906667	0.983	1.09
St Dev	0.013503	0.053075	0.03
T test	9.11E-05	0.001496	5.88E-07
T test Pooled data	9.79E-14	5.47E-13	6.6E-15

Dr Brown
A2 Medial

Measurement	PD (mm)	3DFSPG (mm)	SSFP (mm)
1	1.47	1.47	1.6
2	1.56	1.55	1.57
3	1.65	1.62	1.59
Mean	1.56	1.546667	1.586667
St Dev	0.09	0.075056	0.015275
T test	0.014995	0.007541	7.56E-07
T test Pooled data	4.9E-13	0.000832	3.96E-09

Dr Holland
A2 Lateral

Measurement	PD (mm)	3DFSPG (mm)	SSFP (mm)
1	0.908	0.58	0.793
2	0.904	0.592	0.782
3	0.901	0.595	0.804
Mean	0.904333	0.589	0.793
St Dev	0.003512	0.007937	0.011
T test	0.000127	0.00021	0.076104

Dr Holland
A2 Medial

Measurement	PD (mm)	3DFSPG (mm)	SSFP (mm)
1	1.42	1.63	1.53
2	1.39	1.6	1.5
3	1.42	1.63	1.52
Mean	1.41	1.62	1.516667
St Dev	0.017321	0.017321	0.015275
T test	0.001273	2.53E-07	8.69E-06

Dr Hathcock
A2 Lateral

Measurement	PD (mm)	3DFSPG (mm)	SSFP (mm)
1	0.653	0.63	0.854
2	0.632	0.664	0.951
3	0.637	0.546	0.841
Mean	0.640667	0.613333	0.882
St Dev	0.01097	0.06074	0.060108
T test	0.003726	0.037857	0.02574

Dr Hathcock
A2 Medial

Measurement	PD (mm)	3DFSPG (mm)	SSFP (mm)
1	1.16	1.04	1.31
2	1.18	1.3	1.29
3	1.02	1.27	1.22
Mean	1.12	1.203333	1.273333
St Dev	0.087178	0.142244	0.047258
T test	0.059229	0.444495	0.833701

B1 Lateral

Measurement	Thickness (Pixels)	Thickness (mm)
1	753.054	0.643636
2	798.141	0.682172
3	693.006	0.592313
4	762.053	0.651327
5	693	0.592308
6	807	0.689744
7	789.006	0.674364
8	792.023	0.676943
9	768.006	0.656415
10	756.006	0.646159
Mean	762.9289	0.652076
St Dev	42.06097	0.03595

B1 Medial

Measurement	Thickness (Pixels)	Thickness (mm)
1	513.035	0.438491
2	447.644	0.382602
3	462.243	0.395079
4	511.269	0.436982
5	577.319	0.493435
6	610.66	0.521932
7	642.764	0.549371
8	546.033	0.466695
9	618.029	0.52823
10	654.11	0.559068
Mean	555.1002	0.474445
St Dev	70.21601	0.060014

Dr Brown
B1 Lateral

Measurement	PD (mm)	3DFSPG (mm)	SSFP (mm)
1	0.945	0.793	1.14
2	0.688	0.829	1.09
3	0.688	0.855	0.937
Mean	0.773667	0.825667	1.055667
St Dev	0.148379	0.031134	0.105765
T test	0.286333	0.00171	0.0193
T test Pooled data	0.008728	0.000526	0.004653

Dr Brown
B1 Medial

Measurement	PD (mm)	3DFSPG (mm)	SSFP (mm)
1	1.16	1.35	0.984
2	1.12	1.26	1.12
3	1.19	1.22	1.1
Mean	1.156667	1.276667	1.068
St Dev	0.035119	0.066583	0.07343
T test	1.69E-07	0.000248	0.00117
T test Pooled data	6.95E-08	0.00283	0.000395

Dr Holland
B1 Lateral

Measurement	PD (mm)	3DFSPG (mm)	SSFP (mm)
1	0.64	0.486	0.954
2	0.658	0.517	0.993
3	0.654	0.528	0.973
Mean	0.650667	0.510333	0.973333
St Dev	0.009452	0.021779	0.019502
T test	0.991768	0.000251	5.31E-07

Dr Holland
B1 Medial

Measurement	PD (mm)	3DFSPG (mm)	SSFP (mm)
1	1.31	1.32	1.01
2	1.28	1.35	1.03
3	1.3	1.36	1.06
Mean	1.296667	1.343333	1.033333
St Dev	0.015275	0.020817	0.025166
T test	5.92E-13	1.74E-12	1.99E-09

Dr Hathcock
B1 Lateral

Measurement	PD (mm)	3DFSPG (mm)	SSFP (mm)
1	0.663	0.594	0.88
2	0.558	0.672	0.971
3	0.487	0.57	0.647
Mean	0.569333	0.612	0.832667
St Dev	0.088546	0.053329	0.167106
T test	0.250161	0.337233	0.198321

Dr Hathcock
B1 Medial

Measurement	PD (mm)	3DFSPG (mm)	SSFP (mm)
1	0.673	0.971	0.915
2	0.695	0.923	0.894
3	0.556	0.517	0.634
Mean	0.641333	0.803667	0.814333
St Dev	0.074715	0.249418	0.156526
T test	0.042664	0.149081	0.058706

B2 Lateral

Measurement	Thickness (Pixels)	Thickness (mm)
1	1000.058	0.85475
2	977.029	0.835068
3	994.359	0.849879
4	1031.311	0.881462
5	921.703	0.78778
6	870	0.74359
7	855.047	0.730809
8	864.005	0.738466
9	789.365	0.674671
10	801.679	0.685196
Mean	911.9509	0.779445
St Dev	85.72359	0.073268

B2 Medial

Measurement	Thickness (Pixels)	Thickness (mm)
1	489.009	0.417956
2	522.078	0.446221
3	498.009	0.425649
4	465	0.397436
5	510.035	0.435927
6	468.01	0.400009
7	492.009	0.420521
8	498.036	0.425672
9	510.009	0.435905
10	513.035	0.438491
Mean	494.1231	0.422327
St Dev	20.85184	0.017822

Dr Brown
B2 Lateral

Measurement	PD (mm)	3DFSPG (mm)	SSFP (mm)
1	0.674	0.901	0.72
2	0.682	0.775	0.612
3	0.648	0.832	0.595
Mean	0.668	0.836	0.642333
St Dev	0.017776	0.063095	0.067796
T test	0.001248	0.255246	0.046857
T test Pooled data	0.000329	0.000149	0.00085

Dr Brown
B2 Medial

Measurement	PD (mm)	3DFSPG (mm)	SSFP (mm)
1	1.03	1.1	1.08
2	1.03	1.05	1.12
3	1.11	1.09	1.09
Mean	1.056667	1.08	1.096667
St Dev	0.046188	0.026458	0.020817
T test	0.001277	0.000153	3.37E-05
T test Pooled data	0.00249	0.000548	0.000955

Dr Holland
B2 Lateral

Measurement	PD (mm)	3DFSPG (mm)	SSFP (mm)
1	0.675	0.692	0.693
2	0.695	0.68	0.676
3	0.692	0.665	0.692
Mean	0.687333	0.679	0.687
St Dev	0.010786	0.013528	0.009539
T test	0.003739	0.002214	0.003623

Dr Holland
B2 Medial

Measurement	PD (mm)	3DFSPG (mm)	SSFP (mm)
1	0.889	1.09	1.11
2	0.913	1.11	1.1
3	0.899	1.1	1.14
Mean	0.900333	1.1	1.116667
St Dev	0.012055	0.01	0.020817
T test	1.91E-07	6.04E-10	3.11E-05

Dr Hathcock
B2 Lateral

Measurement	PD (mm)	3DFSPG (mm)	SSFP (mm)
1	0.563	0.605	0.524
2	0.623	0.667	0.5
3	0.483	0.532	0.459
Mean	0.556333	0.601333	0.494333
St Dev	0.070238	0.067575	0.032868
T test	0.012739	0.021659	9.52E-06

Dr Hathcock
B2 Medial

Measurement	PD (mm)	3DFSPG (mm)	SSFP (mm)
1	0.684	0.893	0.828
2	0.504	0.734	0.813
3	0.243	0.712	0.557
Mean	0.477	0.779667	0.732667
St Dev	0.221736	0.098764	0.152317
T test	0.720991	0.02405	0.072139

C1 Lateral

Measurement	Thickness (Pixels)	Thickness (mm)
1	777.006	0.664108
2	714.006	0.610262
3	759.053	0.648763
4	765	0.653846
5	708.915	0.60591
6	768.586	0.656911
7	726.223	0.620703
8	705.517	0.603006
9	727.789	0.622042
10	766.504	0.655132
Mean	746.0962	0.637689
St Dev	28.48539	0.024346

C1 Medial

Measurement	Thickness (Pixels)	Thickness (mm)
1	828.049	0.707734
2	840.434	0.71832
3	868.328	0.742161
4	888.182	0.75913
5	855.258	0.73099
6	843.021	0.720531
7	936.481	0.800411
8	825.136	0.705244
9	903.603	0.77231
10	819.198	0.700169
Mean	851.423	0.727712
St Dev	27.71323	0.023687

Dr Brown
C1 Lateral

Measurement	PD (mm)	3DFSPG (mm)	SSFP (mm)
1	1.01	0.864	1.12
2	0.926	0.843	1.09
3	0.926	0.77	1.15
Mean	0.954	0.825667	1.12
St Dev	0.048497	0.049339	0.03
T test	0.004865	0.016104	0.000203
T test Pooled data	0.001039	0.001687	0.000366

Dr Brown
C1 Medial

Measurement	PD (mm)	3DFSPG (mm)	SSFP (mm)
1	0.892	1.12	1.02
2	1.01	1.19	1.02
3	0.831	1.12	1.02
Mean	0.911	1.143333	1.02
St Dev	0.091	0.040415	0
T test	0.074037	0.000722	5.46E-10
T test Pooled data	2.88E-05	0.000591	0.001722

Dr Holland
C1 Lateral

Measurement	PD (mm)	3DFSPG (mm)	SSFP (mm)
1	1.18	0.89	0.806
2	1.16	0.91	0.835
3	1.2	0.91	0.826
Mean	1.18	0.903333	0.822333
St Dev	0.02	0.011547	0.014844
T test	3.05E-06	8.17E-09	6.21E-06

Dr Holland
C1 Medial

Measurement	PD (mm)	3DFSPG (mm)	SSFP (mm)
1	1.02	1.23	1.19
2	0.961	1.28	1.22
3	1.12	1.29	1.19
Mean	1.033667	1.266667	1.2
St Dev	0.080376	0.032146	0.017321
T test	0.019259	6.11E-05	9.96E-09

Dr Hathcock
C1 Lateral

Measurement	PD (mm)	3DFSPG (mm)	SSFP (mm)
1	0.875	0.8	0.856
2	0.859	0.833	0.817
3	0.67	0.653	0.651
Mean	0.801333	0.762	0.774667
St Dev	0.114019	0.095828	0.108859
T test	0.124395	0.144481	0.152891

Dr Hathcock
C1 Medial

Measurement	PD (mm)	3DFSPG (mm)	SSFP (mm)
1	0.672	1.07	0.999
2	0.656	1.1	0.92
3	0.583	0.908	0.671
Mean	0.637	1.026	0.863333
St Dev	0.047445	0.103286	0.171185
T test	0.053614	0.036296	0.32533

C2 Lateral

Measurement	Thickness (Pixels)	Thickness (mm)
1	461.279	0.394256
2	436.147	0.372775
3	411.962	0.352104
4	376.449	0.321751
5	370.218	0.316426
6	421.807	0.360519
7	360.624	0.308226
8	411.558	0.351759
9	355.269	0.303649
10	369.305	0.315645
Mean	403.5801	0.34494
St Dev	34.23121	0.029257

C2 Medial

Measurement	Thickness (Pixels)	Thickness (mm)
1	1329.487	1.136314
2	1249.042	1.067557
3	1308.88	1.118701
4	1297.53	1.109
5	1377.209	1.177102
6	1338.013	1.143601
7	1347.084	1.151354
8	1299.003	1.110259
9	1245.925	1.064893
10	1263.175	1.079637
Mean	1304.628	1.115066
St Dev	42.7777	0.036562

Dr Brown
C2 Lateral

Measurement	PD (mm)	3DFSPG (mm)	SSFP (mm)
1	0.764	0.706	0.755
2	0.811	0.572	0.675
3	0.696	0.679	0.757
Mean	0.757	0.652333	0.729
St Dev	0.057819	0.070868	0.046776
T test	0.003665	0.012902	0.001934
T test Pooled data	0.002044	0.002843	1.76E-11

Dr Brown
C2 Medial

Measurement	PD (mm)	3DFSPG (mm)	SSFP (mm)
1	1.18	1.09	1.29
2	1.31	1.09	1.18
3	1.33	1.02	1.07
Mean	1.273333	1.066667	1.18
St Dev	0.081445	0.040415	0.11
T test	0.070641	0.153367	0.419351
T test Pooled data	0.000922	0.005509	0.002836

Dr Holland
C2 Lateral

Measurement	PD (mm)	3DFSPG (mm)	SSFP (mm)
1	0.721	0.38	0.552
2	0.721	0.376	0.561
3	0.705	0.368	0.569
Mean	0.715667	0.374667	0.560667
St Dev	0.009238	0.00611	0.008505
T test	2.48E-12	0.006446	4.87E-10

Dr Holland
C2 Medial

Measurement	PD (mm)	3DFSPG (mm)	SSFP (mm)
1	1.21	1.03	1.2
2	1.21	1.11	1.18
3	1.23	1.11	1.22
Mean	1.216667	1.083333	1.2
St Dev	0.011547	0.046188	0.02
T test	1.48E-05	0.350416	0.001582

Dr Hathcock
C2 Lateral

Measurement	PD (mm)	3DFSPG (mm)	SSFP (mm)
1	0.422	0.756	0.547
2	0.542	1.01	0.642
3	0.409	1.11	0.518
Mean	0.457667	0.958667	0.569
St Dev	0.073323	0.182497	0.064861
T test	0.10131	0.026918	0.01996

Dr Hathcock
C2 Medial

Measurement	PD (mm)	3DFSPG (mm)	SSFP (mm)
1	0.88	0.988	1.16
2	1.02	0.764	1.09
3	0.845	0.515	0.917
Mean	0.915	0.755667	1.055667
St Dev	0.092601	0.23661	0.125085
T test	0.057901	0.1177	0.493474

D1 Lateral

Measurement	Thickness (Pixels)	Thickness (mm)
1	789.051	0.674403
2	738.024	0.63079
3	744.024	0.635918
4	813.089	0.694948
5	786.023	0.671815
6	789.023	0.674379
7	798.141	0.682172
8	900	0.769231
9	892.635	0.762936
10	993.018	0.848733
Mean	823.391	0.703753
St Dev	80.32413	0.068653

D1 Medial

Measurement	Thickness (Pixels)	Thickness (mm)
1	687	0.587179
2	579	0.494872
3	654.007	0.55898
4	648.007	0.553852
5	567.389	0.484948
6	603.067	0.515442
7	552	0.471795
8	564.008	0.482058
9	648.007	0.553852
10	726.025	0.620534
Mean	627.9577	0.536716
St Dev	53.72749	0.045921

Dr Brown
D1 Lateral

Measurement	PD (mm)	3DFSPG (mm)	SSFP (mm)
1	0.617	0.678	0.756
2	0.633	0.63	0.726
3	0.634	0.611	0.703
Mean	0.628	0.639667	0.728333
St Dev	0.009539	0.03453	0.026577
T test	0.006397	0.061882	0.391319
T test Pooled data	2.68E-14	5.5E-06	8.88E-06

Dr Brown
D1 Medial

Measurement	PD (mm)	3DFSPG (mm)	SSFP (mm)
1	0.724	0.825	0.921
2	0.792	0.896	0.825
3	0.826	0.9	0.805
Mean	0.780667	0.873667	0.850333
St Dev	0.051936	0.042194	0.062011
T test	0.004146	0.00035	0.00479
T test Pooled data	0.000154	5.72E-08	0.000868

Dr Holland
D1 Lateral

Measurement	PD (mm)	3DFSPG (mm)	SSFP (mm)
1	0.738	0.568	0.718
2	0.739	0.583	0.737
3	0.729	0.588	0.703
Mean	0.735333	0.579667	0.719333
St Dev	0.005508	0.010408	0.017039
T test	0.190745	0.000224	0.545711

Dr Holland
D1 Medial

Measurement	PD (mm)	3DFSPG (mm)	SSFP (mm)
1	0.809	0.802	0.751
2	0.822	0.804	0.763
3	0.811	0.808	0.769
Mean	0.814	0.804667	0.761
St Dev	0.007	0.003055	0.009165
T test	8.89E-09	2.7E-08	4.77E-08

Dr Hathcock
D1 Lateral

Measurement	PD (mm)	3DFSPG (mm)	SSFP (mm)
1	0.583	0.556	0.578
2	0.548	0.654	0.541
3	0.537	0.561	0.529
Mean	0.556	0.590333	0.549333
St Dev	0.024021	0.055194	0.025541
T test	0.000165	0.040407	0.000158

Dr Hathcock
D1 Medial

Measurement	PD (mm)	3DFSPG (mm)	SSFP (mm)
1	0.56	0.724	0.709
2	0.618	0.711	0.682
3	0.572	0.711	0.576
Mean	0.583333	0.715333	0.655667
St Dev	0.030616	0.007506	0.070302
T test	0.077803	5.13E-07	0.076733

D2 Lateral

Measurement	Thickness (Pixels)	Thickness (mm)
1	765.376	0.654168
2	753.597	0.6441
3	726.75	0.621154
4	693.785	0.592979
5	742.026	0.63421
6	738.39	0.631103
7	667.323	0.570362
8	786.092	0.671874
9	726.099	0.620597
10	783.092	0.669309
Mean	745.3597	0.63706
St Dev	27.96201	0.023899

D2 Medial

Measurement	Thickness (Pixels)	Thickness (mm)
1	1144.275	0.978013
2	1091.79	0.933154
3	1105.971	0.945274
4	1132.435	0.967893
5	1059.718	0.905742
6	1101.2	0.941197
7	1212.728	1.03652
8	1210.075	1.034252
9	1217.35	1.04047
10	1233.157	1.05398
Mean	1139.717	0.974117
St Dev	60.17079	0.051428

Dr Brown
D2 Lateral

Measurement	PD (mm)	3DFSPG (mm)	SSFP (mm)
1	0.75	0.689	0.805
2	0.755	0.708	0.804
3	0.761	0.712	0.737
Mean	0.755333	0.703	0.782
St Dev	0.005508	0.012288	0.038974
T test	2.46E-07	0.000195	0.010033
T test Pooled data	5.45E-13	1.17E-18	0.000897

Dr Brown
D2 Medial

Measurement	PD (mm)	3DFSPG (mm)	SSFP (mm)
1	0.924	1.13	0.973
2	0.61	0.939	0.913
3	0.652	0.877	0.966
Mean	0.728667	0.982	0.950667
St Dev	0.170462	0.131867	0.032808
T test	0.118257	0.984889	0.244286
T test Pooled data	0.008713	0.008096	0.000194

Dr Holland
D2 Lateral

Measurement	PD (mm)	3DFSPG (mm)	SSFP (mm)
1	0.785	0.793	0.788
2	0.799	0.809	0.803
3	0.787	0.787	0.768
Mean	0.790333	0.796333	0.786333
St Dev	0.007572	0.011372	0.017559
T test	1.73E-08	7.37E-08	2.07E-05

Dr Holland
D2 Medial

Measurement	PD (mm)	3DFSPG (mm)	SSFP (mm)
1	0.853	0.811	1.1
2	0.849	0.83	1.11
3	0.869	0.834	1.04
Mean	0.857	0.825	1.083333
St Dev	0.010583	0.012288	0.037859
T test	2.49E-05	3.21E-06	0.016959

Dr Hathcock
D2 Lateral

Measurement	PD (mm)	3DFSPG (mm)	SSFP (mm)
1	0.628	0.637	0.607
2	0.596	0.61	0.694
3	0.583	0.639	0.604
Mean	0.602333	0.628667	0.635
St Dev	0.023159	0.016197	0.051118
T test	0.153054	0.87086	0.907271

Dr Hathcock
D2 Medial

Measurement	PD (mm)	3DFSPG (mm)	SSFP (mm)
1	0.529	0.721	0.67
2	0.507	0.638	0.739
3	0.462	0.48	0.605
Mean	0.499333	0.613	0.671333
St Dev	0.034152	0.12243	0.06701
T test	4.32E-06	0.028769	0.006339

E1 Lateral

Measurement	Thickness (Pixels)	Thickness (mm)
1	882.326	0.754125
2	919.102	0.785557
3	950.091	0.812044
4	942.936	0.805928
5	891.182	0.761694
6	837.048	0.715426
7	861.084	0.735969
8	846.261	0.7233
9	850.038	0.726528
10	786.572	0.672284
Mean	874.2604	0.747231
St Dev	52.34316	0.044738

E1 Medial

Measurement	Thickness (Pixels)	Thickness (mm)
1	846.048	0.723118
2	792.091	0.677001
3	864.047	0.738502
4	825	0.705128
5	801.006	0.684621
6	819.005	0.700004
7	822.005	0.702568
8	804.09	0.687256
9	807.089	0.68982
10	837.65	0.71594
Mean	821.5031	0.702139
St Dev	22.3459	0.019099

Dr Brown
E1 Lateral

Measurement	PD (mm)	3DFSPG (mm)	SSFP (mm)
1	0.896	1.04	0.774
2	0.872	0.984	0.768
3	0.825	1.18	0.768
Mean	0.864333	1.068	0.77
St Dev	0.036116	0.100955	0.003464
T test	0.010246	0.026452	0.169681
T test Pooled data	0.000311	0.003148	8.76E-05

Dr Brown
E1 Medial

Measurement	PD (mm)	3DFSPG (mm)	SSFP (mm)
1	1.07	1.19	1.1
2	1.1	1.16	1.07
3	1.07	1.17	1.03
Mean	1.08	1.173333	1.066667
St Dev	0.017321	0.015275	0.035119
T test	1.39E-05	1.17E-06	0.001532
T test Pooled data	0.002398	2.61E-05	0.001236

Dr Holland
E1 Lateral

Measurement	PD (mm)	3DFSPG (mm)	SSFP (mm)
1	0.782	0.884	0.637
2	0.82	0.904	0.649
3	0.83	0.892	0.637
Mean	0.810667	0.893333	0.641
St Dev	0.025325	0.010066	0.006928
T test	0.022052	1.13E-06	1.7E-05

Dr Holland
E1 Medial

Measurement	PD (mm)	3DFSPG (mm)	SSFP (mm)
1	0.935	1.12	1.08
2	0.96	1.12	1.1
3	0.936	1.13	1.08
Mean	0.943667	1.123333	1.086667
St Dev	0.014154	0.005774	0.011547
T test	6.94E-06	4.56E-15	1.97E-08

Dr Hathcock
E1 Lateral

Measurement	PD (mm)	3DFSPG (mm)	SSFP (mm)
1	0.658	0.858	0.63
2	0.551	1.06	0.571
3	0.529	1.16	0.525
Mean	0.579333	1.026	0.575333
St Dev	0.06901	0.153844	0.052634
T test	0.038365	0.086043	0.01518

Dr Hathcock
E1 Medial

Measurement	PD (mm)	3DFSPG (mm)	SSFP (mm)
1	1.01	1.15	1.07
2	0.889	1.13	0.993
3	0.657	1.08	0.846
Mean	0.852	1.12	0.969667
St Dev	0.179385	0.036056	0.113808
T test	0.285245	0.001227	0.054336

E2 Lateral

Measurement	Thickness (Pixels)	Thickness (mm)
1	756.292	0.646403
2	774.145	0.661662
3	810	0.692308
4	831.087	0.710331
5	873.046	0.746193
6	831	0.710256
7	732.006	0.625646
8	747.006	0.638467
9	735.006	0.62821
10	816.199	0.697606
Mean	800.4781	0.684169
St Dev	44.96381	0.038431

E2 Medial

Measurement	Thickness (Pixels)	Thickness (mm)
1	729.099	0.623162
2	681.423	0.582413
3	684.237	0.584818
4	690.059	0.589794
5	693	0.592308
6	717.006	0.612826
7	684.007	0.584621
8	699.058	0.597485
9	720.225	0.615577
10	706.435	0.603791
Mean	703.7548	0.6015
St Dev	16.58956	0.014179

Dr Brown
E2 Lateral

Measurement	PD (mm)	3DFSPG (mm)	SSFP (mm)
1	0.797	0.982	0.869
2	0.698	1.05	0.755
3	0.605	0.91	0.759
Mean	0.7	0.980667	0.794333
St Dev	0.096016	0.07001	0.064694
T test	0.707459	0.0108	0.072317
T test Pooled data	0.00191	0.003851	0.000783

Dr Brown
E2 Medial

Measurement	PD (mm)	3DFSPG (mm)	SSFP (mm)
1	1.6	1.21	1.31
2	1.25	1.17	1.1
3	1.17	1.3	0.863
Mean	1.34	1.226667	1.091
St Dev	0.228692	0.066583	0.223636
T test	0.03016	0.003346	0.062235
T test Pooled data	0.00359	8.05E-05	0.006666

Dr Holland
E2 Lateral

Measurement	PD (mm)	3DFSPG (mm)	SSFP (mm)
1	0.707	0.752	0.729
2	0.717	0.73	0.734
3	0.724	0.746	0.705
Mean	0.716	0.742667	0.722667
St Dev	0.008544	0.011372	0.015503
T test	0.015043	0.00079	0.014476

Dr Holland
E2 Medial

Measurement	PD (mm)	3DFSPG (mm)	SSFP (mm)
1	1.1	1.21	0.976
2	1.12	1.23	0.979
3	1.12	1.23	1.03
Mean	1.113333	1.223333	0.995
St Dev	0.011547	0.011547	0.030348
T test	2.47E-07	1.11E-07	0.001065

Dr Hathcock
E2 Lateral

Measurement	PD (mm)	3DFSPG (mm)	SSFP (mm)
1	0.551	0.789	0.636
2	0.521	0.97	0.727
3	0.5	0.676	0.597
Mean	0.524	0.811667	0.653333
St Dev	0.025632	0.148305	0.066711
T test	0.000361	0.251586	0.627801

Dr Hathcock
E2 Medial

Measurement	PD (mm)	3DFSPG (mm)	SSFP (mm)
1	1.24	1.25	1.17
2	1.18	1.18	1.11
3	1.03	1.15	0.85
Mean	1.15	1.193333	1.043333
St Dev	0.108167	0.051316	0.170098
T test	0.012243	0.002024	0.045203

F1 Lateral

Measurement	Thickness (Pixels)	Thickness (mm)
1	594.348	0.50799
2	626.26	0.535265
3	617.111	0.527445
4	606.898	0.518716
5	615.731	0.526266
6	621.007	0.530775
7	627.029	0.535922
8	654.028	0.558998
9	654.11	0.559068
10	579.117	0.494972
Mean	618.9617	0.529027
St Dev	23.2845	0.019901

F1 Medial

Measurement	Thickness (Pixels)	Thickness (mm)
1	609.738	0.521144
2	792.023	0.676943
3	819.005	0.700004
4	777.006	0.664108
5	783.006	0.669236
6	780.092	0.666745
7	831.049	0.710298
8	807.557	0.69022
9	838.552	0.716711
10	844.541	0.72183
Mean	783.1612	0.669369
St Dev	65.76595	0.05621

Dr Brown
F1 Lateral

Measurement	PD (mm)	3DFSPG (mm)	SSFP (mm)
1	0.592	1.09	0.668
2	0.587	1.07	0.821
3	0.632	1.17	0.753
Mean	0.603667	1.11	0.747333
St Dev	0.024664	0.052915	0.076657
T test	0.019887	0.001943	0.036563
T test Pooled data	1.23E-05	1.24E-08	0.000824

Dr Brown
F1 Medial

Measurement	PD (mm)	3DFSPG (mm)	SSFP (mm)
1	1.12	1.44	1.14
2	1.12	1.44	1.17
3	1.11	1.37	1.19
Mean	1.116667	1.416667	1.166667
St Dev	0.005774	0.040415	0.025166
T test	7.51E-10	2.87E-06	1.11E-08
T test Pooled data	2.08E-05	0.000145	1.04E-05

Dr Holland
F1 Lateral

Measurement	PD (mm)	3DFSPG (mm)	SSFP (mm)
1	0.648	0.985	0.705
2	0.644	0.998	0.723
3	0.626	1.01	0.717
Mean	0.639333333	0.99766667	0.715
St Dev	0.011718931	0.01250333	0.009165151
T test	2.15771E-05	1.6813E-08	1.32599E-08

Dr Holland
F1 Medial

Measurement	PD (mm)	3DFSPG (mm)	SSFP (mm)
1	1.14	1.29	1.2
2	1.14	1.32	1.18
3	1.12	1.29	1.18
Mean	1.133333333	1.3	1.186666667
St Dev	0.011547005	0.01732051	0.011547005
T test	1.36278E-10	8.7452E-12	4.28427E-11

Dr Hathcock
F1 Lateral

Measurement	PD (mm)	3DFSPG (mm)	SSFP (mm)
1	0.525	0.925	0.629
2	0.582	0.967	0.619
3	0.55	0.843	0.573
Mean	0.552333	0.911667	0.607
St Dev	0.028572	0.063066	0.029866
T test	0.299147	0.007513	0.033011

Dr Hathcock
F1 Medial

Measurement	PD (mm)	3DFSPG (mm)	SSFP (mm)
1	0.88	1.16	1.12
2	1	1.23	1
3	0.904	1.11	0.968
Mean	0.928	1.166667	1.029333
St Dev	0.063498	0.060277	0.080133
T test	0.00786	0.000796	0.008345